

Experimental Investigation of Flow in Channels with Extended Boundaries

M. Kamal¹, Ehab M. Fattouh², M. Mokhtar³, S. Ead⁴

¹(PhD Researcher), ²(Associate Professor), ³(Assistant Professor), ⁴(Professor of Hydraulics)
Irrigation and Hydraulics Department, Faculty of Engineering, Ain Shams University, Cairo, Egypt

Abstract: Pipe flow and open channel flow have been thoroughly studied in past years. In this paper, a new type of flow called Flow in Channels with Extended Boundaries was introduced and experimentally investigated. In this flow, the channel sides are extended to cover part of the free surface. The extensions just touch the flow, so the pressure on the top surface is still approximately atmospheric. The existence of fixed extended boundaries affects the distributions of both velocity and discharge. Three cases with boundaries extension ratios = 25%, 50%, and 67% along with a typical open channel flow case, were examined. Acoustic Doppler Velocimeters were used to sample the velocity data through a complete mesh to create iso-lines of velocity distribution. For the case of open channel flow, results showed that the effect of the side boundaries was negligible and the velocity distribution at the centerline matched well with Prandtle power law ($N = 6$). For the discharge distribution, the first 25% of the flow area, near the side boundary, passed only 18.64% of the total discharge. In cases of Flow in Channels with Extended Boundaries, a low velocity zone bounded by the extension, the flume bed and the side wall, was formed. The iso-lines of velocity distribution in this zone resembled the case of pipe flow, but were not closed due to the absence of the fourth boundary. The measured velocity data at the centerline matched well with Prandtle power law at $N = 12$. The discharges passing in the low velocity zones of the three cases with boundaries extension ratios = 25%, 50%, and 67% were less than that of the open channel flow case by 7.36%, 4.21%, and 2.79%, respectively.

Key words: Flow in Channels with Extended Boundaries, Iso-lines of Velocity Distribution, Acoustic Doppler Velocimeter, Discharge Distribution.

Date of Submission: 28-03-2020

Date of Acceptance: 16-04-2020

I. Introduction And Literature Review

Pipe Flow (PF) and Open Channel Flow (OCF) have been thoroughly studied through decades of development of hydraulic engineering science. In PF, flow is contained in a closed conduit, and is mainly due to losses in pressure head. In OCF, the top surface is the free surface, and the flow is driven by the bed slope in the flow direction. However, in many environmental engineering applications, a new type of flow called the "Flow in Channels with Extended Boundaries (FCEB)" is experienced. In FCEB, the channel boundaries are extended to cover part of the free surface. From the hydraulic point of view, the extensions just touch the flow, so the pressure on the top surface is still *approximately* atmospheric. The existence of a stagnant extension affects the distribution of velocity and consequently other flow characteristics. Examples of applications of FCEB in the field of environmental engineering are the flows in channels with floating wetland, floating jetties and marinas, floating solar cells, and floating ice layers (See Photo no 1). Other applications involve the floating weeds and floating dirt islands.

Wetlands are widely used as they show good performance in improving stream water quality. The idea is to use the biological and chemical actions of some plants to decrease the concentration of the undesirable elements in water courses through pre-calculated wetland dimensions and plant density. Recently, plants are cultivated as floating wetlands on the surface of water streams sustained by specially-made nets. The nets project as extensions to the side boundaries, covering part of the stream, and just touching the free surface. Floating jetties and marinas project as extensions to the side boundaries, and are used for mooring of small boats and getting fun setting across the water channel. Solar cells are sometimes installed on floating structures projecting as extensions to the side boundaries of artificial or natural streams. This decreases stream evaporation losses, saves areas required to install solar cells for other purposes, and harvests the solar energy to generate electric power. In cold countries, streams are covered with layers of ice that form an extension to the boundaries partially covering the free surface.

In all the aforementioned applications, the pressure at the stream surface is still approximately atmospheric as the floating structure just touches the top surface. However, both the velocity and discharge distributions are severely affected. The flow in any of these cases is called FCEB.

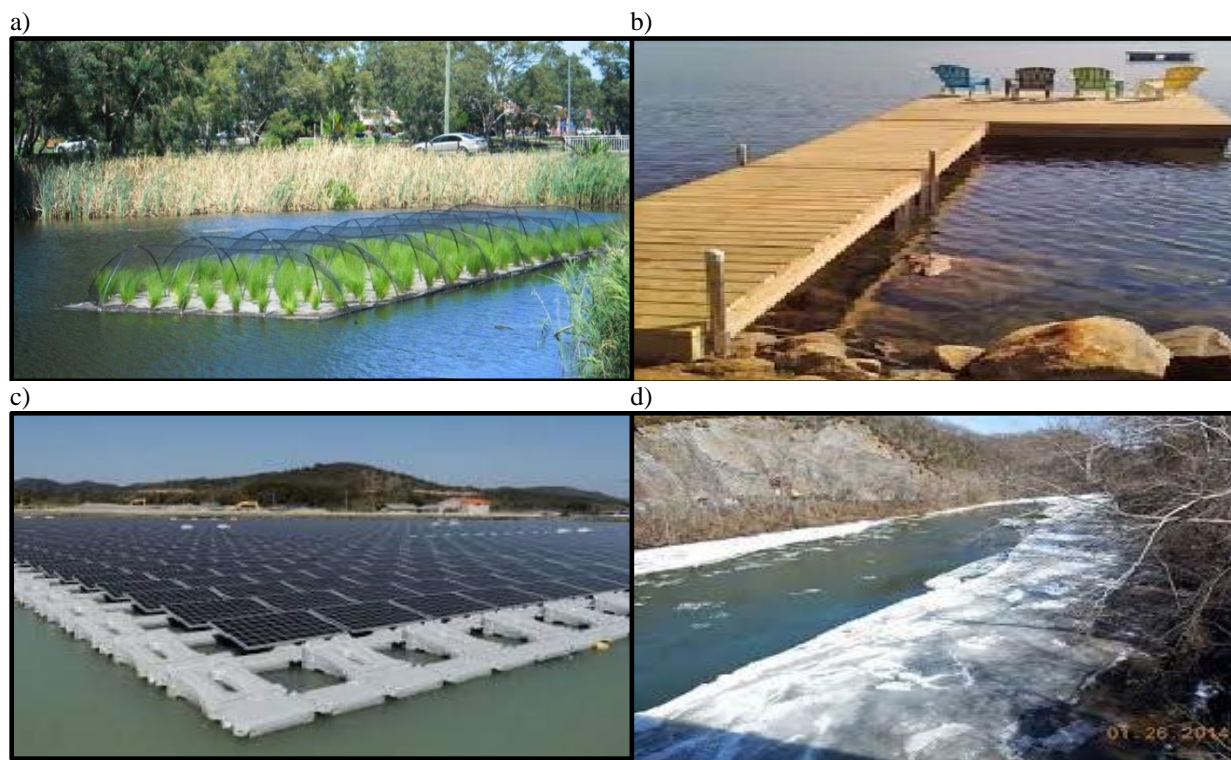


Photo no 1: Channels with floating a) Wetland, b) Jetties and Marinas, c) Solar Sells, d) Ice Layers

In published engineering and research works, one may find many attempts to study the characteristics of the above mentioned applications. Examples are; studies to optimize the dimensions of floating wetlands for best water quality, dimensions of jetties and marinas for more moored boats and dimensions of solar cells to harvest more energy, and studies for the formation and crystallization of ice layers. However, only very few attempts are found in studying the hydraulics of flow in streams where these applications are used.

This study is an experimental investigation of the FCEB in a laboratory flume where the two side boundaries are extended. The Doppler effects through Acoustic Doppler Velocimeter (ADV) are used to sample the velocity data through a complete mesh to create iso-lines of velocity distribution of the FCEB. Available, in the literature, there exist published research works in the fields of investigating the velocity distribution in OCF using analytical, numerical, and measuring techniques. Some research works are introduced hereafter.

Rasoul et al.¹² used Laser Doppler Anemometer (LDA) to sample the velocity distribution obstructed by staggered cylinders. They used the experimental data to verify the flow domain calculated by solving the Navier-Stokes equations together with the continuity equation using Finite Difference Method. González et al.³ collected data of two-dimensional velocity distribution with a fixed Acoustic Doppler Current Profiler. They compared measured velocity distribution data with the logarithmic-law and power-law velocity distributions. Voulgaris and Trowbridge¹⁶ undertook simultaneous experimental measurements in a laboratory flume to collect velocity and turbulence data using ADV and LDA. They reported that the two sets of velocity data agreed well. However, when calculating the turbulence shear based on the turbulence data of the two devices, they noticed considerable variation. Kundu and Ghoshal⁶ combined the log-law for inner region and parabolic-law for relatively strong outer region to deduce an explicit equation for the velocity distribution based on the experimental data. Lassabatere et al.⁷ used analytical approach to present a solution for the Reynolds-Averaged Navier-Stokes equations for the determination of the distribution of the stream-wise velocity in both rough and smooth flow regimes, and compared it with the experimental data. Monteroa et al.⁹ in preprocessing the ADV pings, extended the techniques available in literature by incorporating spatial and temporal averaging (filtering) processes in the analysis. They developed a conceptual model, simulating the flow field with Direct Numerical Simulation (DNS) and ADV sampling. Ruonan et al.¹³ designed a Particle Images Velocimeter (PIV) to check the ADV velocity and turbulence data measured. Pradhan et al.¹¹ used series of Pitot tubes to measure the velocity distribution in an experimental meandering channel with a sine-generated curvature in cases of smooth and rough boundaries. Yang et al.¹⁷ considered water-surface velocities detected by UHF radar as boundary conditions and derived a new velocity distribution model based on the Reynolds-Averaged Navier-Stokes equations. They reported that their model was superior to the power law model, especially near the side wall. Kumbhakar et al.⁵ derived explicit analytical solutions for the vertical and transverse distribution of stream-wise velocity using the concept of the maximum entropy (MaxEnt) principle.

Very few research works were conducted in the hydraulic investigation of FECB. These researches were conducted as side studies for Ice Rivers. Tang and Davar¹⁵ studied experimentally the case of flow in rivers partially covered with ice. They studied five models with five different coverage ratios. They tested the case of completely open channel for comparison. They used Manning equation and Streeter logarithmic form of velocity distribution in their analysis. Mitchell⁸ focused on the distribution of velocity of flow in the stream under the ice layers. He calculated the equivalent Manning coefficient of roughness for the stream boundaries and ice. He used the equation of Shen and Ackermann¹⁴ to calculate the discharge distribution along the flow section. In the present study, the FCEB is simulated experimentally and the so-called new ADV system as defined in Kamal⁴ is used to collect velocity data to investigate the flow. It is expected that this research work would give a new insight to researchers and engineers in the field of hydraulic engineering.

II. Theoretical Considerations

The study measurements resulted in complete iso-lines mesh of the velocity distribution. Nezu and Rodi¹⁰ showed that the flow is strongly dependent on the aspect ratio, $a = b/Y$, where b is the channel width and Y is the flow depth. The channel is said to be narrow if $a \leq 5$, where secondary currents due to sidewall result in a “dip” in the velocity distribution near the surface such that the maximum velocity is below the water surface. If $a > 5$, the channel is wide and secondary currents may be neglected especially near the channel center. For velocity distribution in the vertical direction, González et al.³ identified the following regions in smooth channels:

- **Region (1):** This region is located near the channel bed where $y \leq 0.2Y$ (y is the vertical distance from the bed). The flow velocity (u) at a vertical distance (y) follows the law of the wall:

$$\frac{u}{u_*} = f\left(\frac{yu_*}{\nu}\right) \quad (1)$$

where u_* is the shear velocity $= (\tau/\rho)^{0.5}$, τ is the bed shear stress, ρ is the fluid mass density, and ν is the fluid kinematic viscosity. Researches on the function, f showed that equation (1) takes the following form:

$$\frac{u}{u_*} = \frac{1}{k} \ln\left(\frac{yu_*}{\nu}\right) + c_1 \quad (2)$$

where k is the Von-Karman constant = 0.39 to 0.41, and c_1 was determined experimentally as 5.1 to 5.7. Very close to the wall, when y approaches zero, and referring to the basic relation, $\tau = \mu \frac{\partial u}{\partial y}$, it can be shown that:

$$\frac{u}{u_*} \approx \frac{yu_*}{\nu} \quad (3)$$

- **Region (2):** This region is located near the free surface where $0.6Y \leq y \leq Y$. Denoting u_{max} as the maximum velocity, The relation reads:

$$\frac{u}{u_{max}} = f\left(\frac{y}{Y}\right) \quad (4)$$

- **Region (3):** For the intermediate region where $0.2Y < y < 0.6Y$, many relations are found in the literature.
- It is usually assumed that the Prandtl power law describes the velocity distribution all over the entire flow depth. The Prandtl power law reads:

$$\frac{u}{u_{max}} = \left(\frac{y}{Y}\right)^{\frac{1}{N}} \quad (5)$$

where N is an exponent varies from 4 to 12, and Chanson¹ recommended that $N = 6$ for smooth channels.

- In case of channels with rough beds, the roughness height (k_s) is used as a length scale:

$$\frac{u}{u_*} = \frac{1}{k} \ln\left(\frac{y}{k_s}\right) + c_2 \quad (6)$$

where c_2 is a constant to be determined experimentally.

- Another approach was given by Chen² who introduced a power relation for the entire depth as follows:

$$\frac{u}{u_*} = C_3 \left(\frac{y}{y'}\right)^{C_4} \quad (7)$$

where y' is a vertical distance where u is equal to zero ($y' = k_s/30$), and C_3 and C_4 are constants to be determined experimentally.

III. Experimental Work

In this section, details of the flume, the measuring devices, the test models, and the experimental data, are introduced.

1. The Flume: High Density Overlay Plywood (HDOP) was used to construct the flume's bed and walls as in Photo no 2. The flume is of a rectangular recirculating type. Its length is 14 m, width is 1.2 m, and depth is 1.0 m. Four longitudinal timber girders (5 cm × 25 cm) sustain the weights of the flume and the flowing water. Transvers joists, spaced 0.3 m, transmit the weight of the HDOP base to the longitudinal girders. Seams were sealed using waterproof adhesive sealant made of polyurethane. In the new ADV system used in this

experimental work, manual carriage is replaced by an automatically-moving transverse mechanism, where the sampling locations of the ADV are preset and fed to the computer control unit through x-y mesh (Photo no 3 and see Kamal⁴ for details). The position of the cross section in stream direction is fixed manually.



Photo no 2: Timber flume during construction



Photo no 3: The automotive carriage

2. The Measuring Devices: Acoustic Doppler Velocimeters (ADV) were used to sample velocity data in cross sections perpendicular to the flow direction. The ADVs used were down-looking Nortek Vectrino II profiler ADV (3000 samples per min, 3 min sampling per position, 100 Hz frequency, and 0 to 150 cm/s velocity range), and Nortek Vectrino+ side-looking ADV (3000 samples per min, 3 min sampling per position, 200 Hz frequency, and 0 to 150 cm/s velocity range). Each ADV consists of three main parts; transmitter and four receivers, flexible stem, and ADV processing unit (See Photo no 4). Down-looking Nortek Vectrino II profiler ADV (See Photo 5) was used in down and side-looking directions to benefit from its capability to sample up to 30, 1 mm thick, cells and not just a sample as in the case of Nortek Vectrino+ side-looking ADV. On the other hand, Nortek Vectrino+ side-looking ADV was used in the up-looking direction (See Photo no 6). The processors of the two ADV types store data in data files with extensions *.ntk and *.vno for Nortek Vectrino II profiler and NorTek Vectrino+, respectively. The new MatLab Code for ADV data Post-processing (MCAP) was used for post-processing and de-spiking data files (See Kamal⁴).

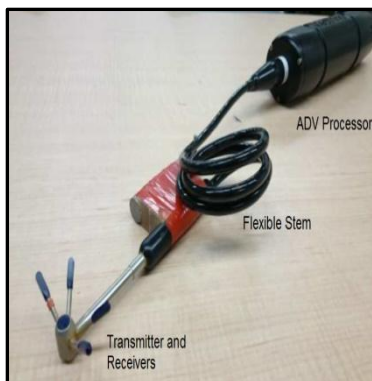


Photo no 4: ADV



Photo no 5: Down-Looking ADV in Down-Looking orientation



Photo no 6: Side-Looking ADV in Up-Looking orientation

3. The Test Models: Figure no 1 shows the test models installed in the laboratory flume. The two parts of the model, made from HDOP with widths X1 and X2, were installed as extensions to the two channel side boundaries. Model parts are fixed just touching the flow free surface and extended all along the entire flume length to simulate the case of FCEB. Four experiments were conducted. The aspect ratio was kept constant ($a = b/Y = 10$) as the flow depth was kept constant ($Y = 120$ mm). The first experiment was performed under the OCF conditions where boundaries extension ratios, $BER = (X1+X2)/b = 0$ for the sake of comparison. In the second, third, and fourth experiments, the values of BER were equal to 25%, 50%, and 67% and the values of $X1=X2$ were equal to 150 mm, 300 mm, and 402 mm, respectively. Photo no 7 shows the installation of extensions in the fourth experiment (symmetric $BER = 67%$, $X1 = X2 = 402$ mm). Many factors are expected to affect the flow characteristics such as; boundary-related factors (boundaries extension widths X1 and X2, flume

width b , roughness of channel boundaries, roughness of contact surface of extensions, etc.), and flow factors (flow depth, flow velocity, etc.). Applying the dimensional analysis technique, it can be shown that:

$$\frac{u}{u_{max}} = f\left(\frac{X1+X2}{b}, F, \frac{y}{Y}\right) \quad (8)$$

where F is the Froude number, and the effect of roughness was neglected due to the smoothness of HDOP.

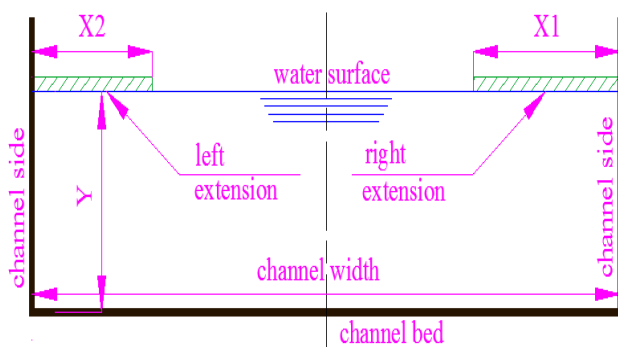


Figure no 1: Test models installed in the laboratory flume



Photo no 7: Symmetric BER = 67%

Figure no 2 shows the sampling locations for ADV data collection. The down-looking Nortek Vectrino II profiler ADV was used in two different orientations as mentioned earlier; side looking orientation (yellow circles), and down-looking orientation (red circles). Blue circles represent up-looking orientation of the Nortek Vectrino+ side-looking ADV. 196 positions (1,764,000 readings) are sampled in the first experiment and 190 positions (1,710,000 readings) are sampled in any of the other three experiments:

- The section was divided into measuring columns 50 mm apart,
- Near boundaries, the distances between measuring columns were decreased to about 15 mm, and
- Two no-data areas ($x = 50$ mm and $y = 45$ mm) existed in the channel corners.

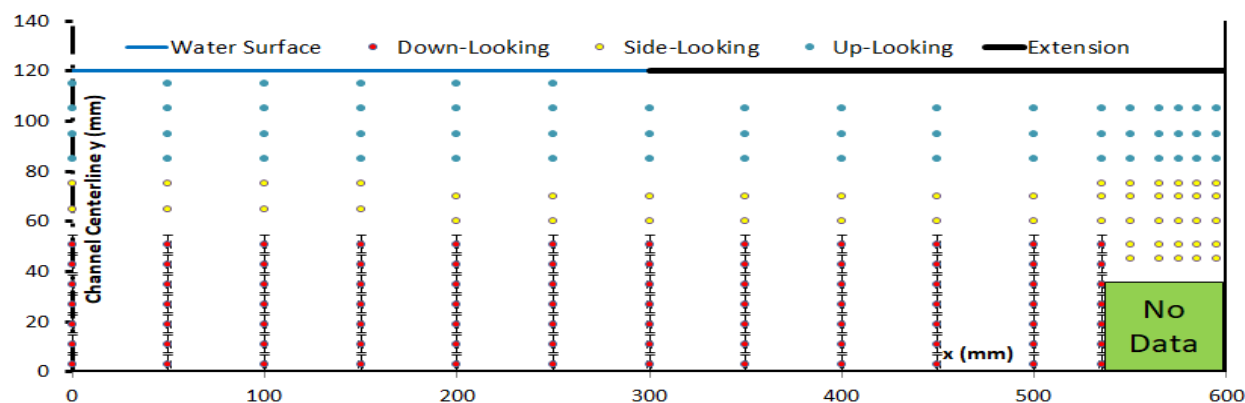


Figure no 2: ADV Sampling Locations

4. Experimental Data: Figures no 3, 4, 5, and 6 give the iso-line flow velocity distributions in the flow cross sections in cases of smooth boundaries and symmetric BER = 0%, 25%, 50%, and 67%, respectively. The values of the flow velocity (u) normalized by the average flow velocity (U) are represented using both colors and labeled iso-lines. Proved symmetric by the preliminary runs, ADV data was collected in only half of the flow cross section. The other two velocity components together with the three turbulence components measured by ADV were found negligible. Due to the limitations of ADV capabilities, a no-data area existed in the flume corner.

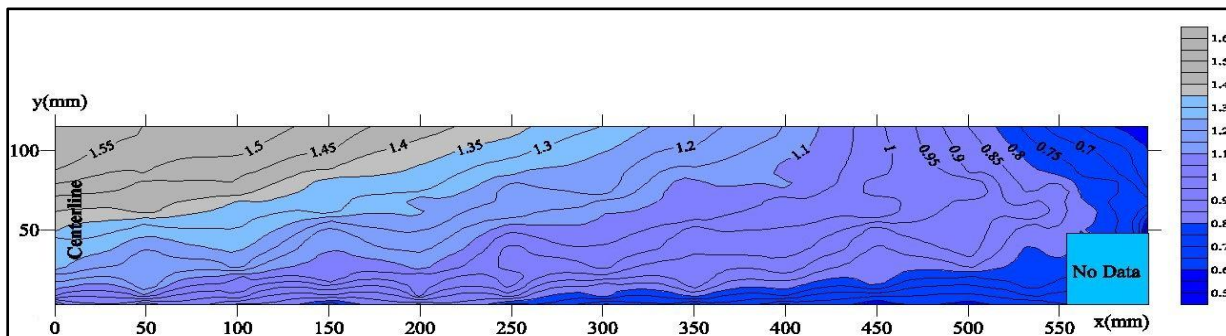


Figure no 3: Iso-lines for relative velocity u/U (BER = 0%)

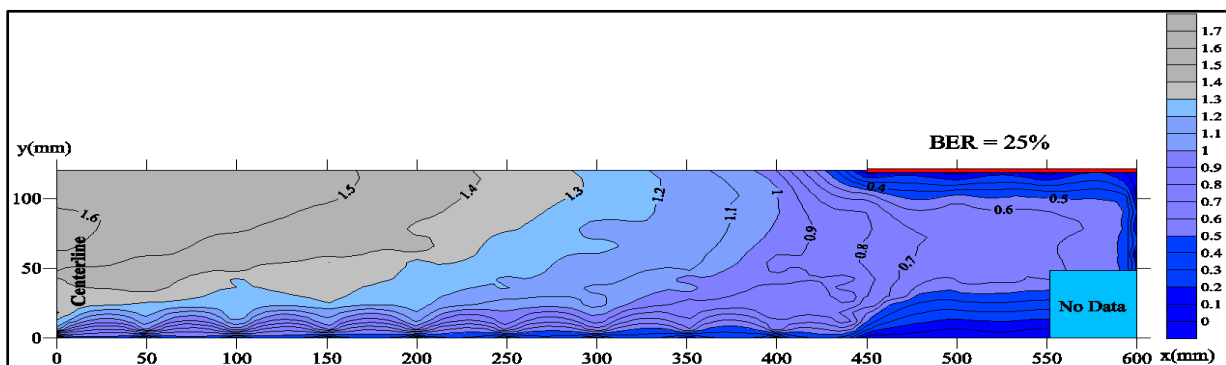


Figure no 4: Iso-lines for relative velocity u/U (BER = 25%)

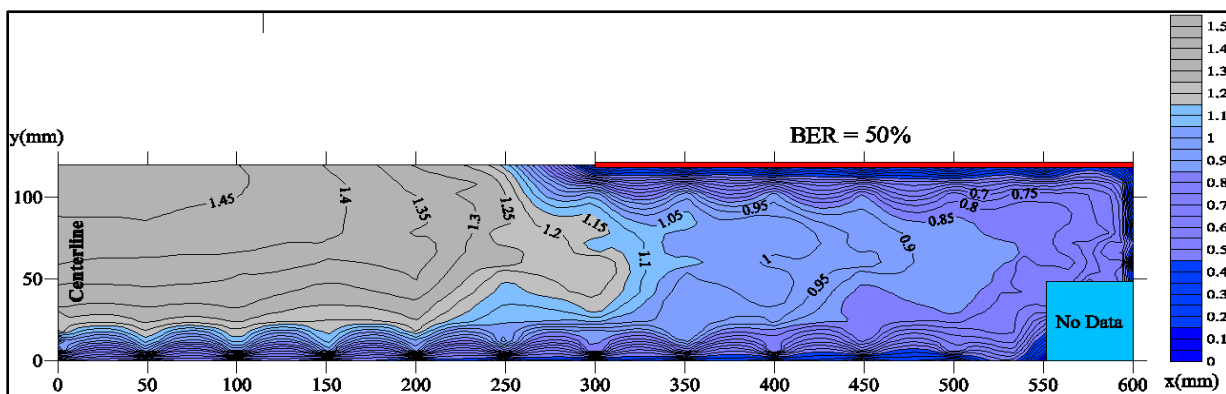


Figure no 5: Iso-lines for relative velocity u/U (BER = 50%)

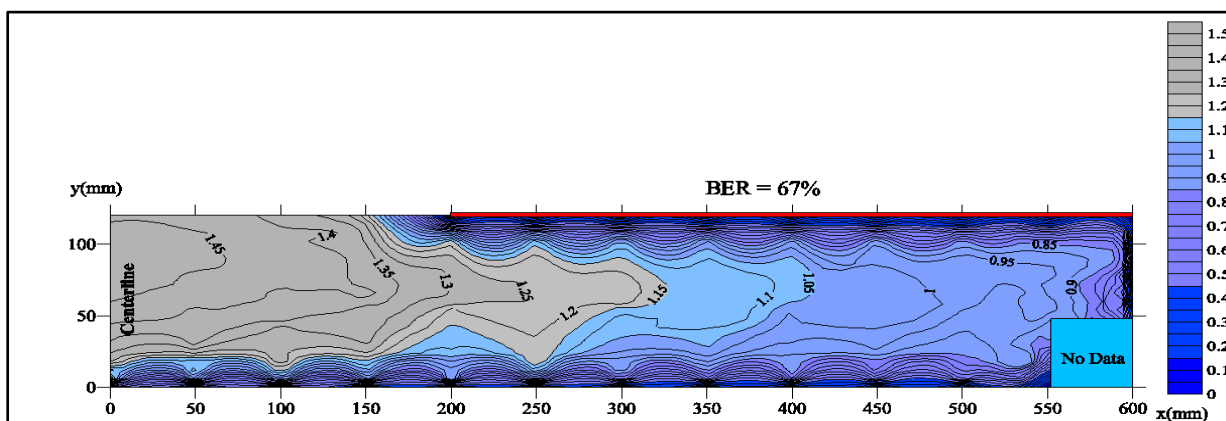


Figure no 6: Iso-lines for relative velocity u/U (BER = 67%)

IV. Analysis and Discussion

1. **Case of BER = 0%:** This is the case of OCF, which is experimentally investigated to be used for comparison as a reference case and to check the accuracy of the ADV system used against equations available in the literature. Many researchers compared their ADV data with known equations or other experimental data collected using other velocity measuring devices (see Chen², Ruonan et al.¹³ and Voulgaris and Trowbridge¹⁶). The measured data showed that the maximum normalized flow velocity (u/U) was equal to 1.59, and was located at the centerline where the vertical distance (y) was equal to $0.875Y$. The following may be noticed in Figure 3:

- The velocity is minimum near the boundaries and maximum at the channel centerline.
- The aspect ratio, $a = 1200/120 = 10 > 5$, and the iso-lines near the centerline show the negligible small effects of the channel sides. This matches well with what was reported by Nezu and Rodi¹⁰ for wide channels ($a > 5$).
- The density of the iso-lines is relatively high close to the boundaries where the velocity damps very rapidly because of the boundary effects.
- The small damping distance indicates that the depth of the boundary layer is relatively small which is reasonable as the flume boundaries are made of plywood (rather smooth material with small height of absolute roughness).

Figure no. 7 shows the change of the relative flow velocity (u/u_{max}) with the relative vertical distance (y/Y), where u_{max} is the maximum velocity recorded. Markers show the relative velocity distributions at different relative x (where relative $x = x/0.5b$ where $0.5b = 600$ mm), and the solid line is drawn using equation no 5 with $N = 6$ following Chanson¹ recommendations. The following may be outlined:

- Good match is noticed between equation 5 and the measured data at the centerline (relative $x = 0$).
- With the increase of relative x , the deviation between equation 5 and the measured data increases due to the effects of the side boundary.
- Still, at relative $x = 0.99$, the relative velocity (u/u_{max}) is about 0.4. This indicates that the side boundary layer is small due to the smoothness of HDOP.
- The discussion of Figures no 3 and 7 showed that the measurements of ADV system are fairly accurate.

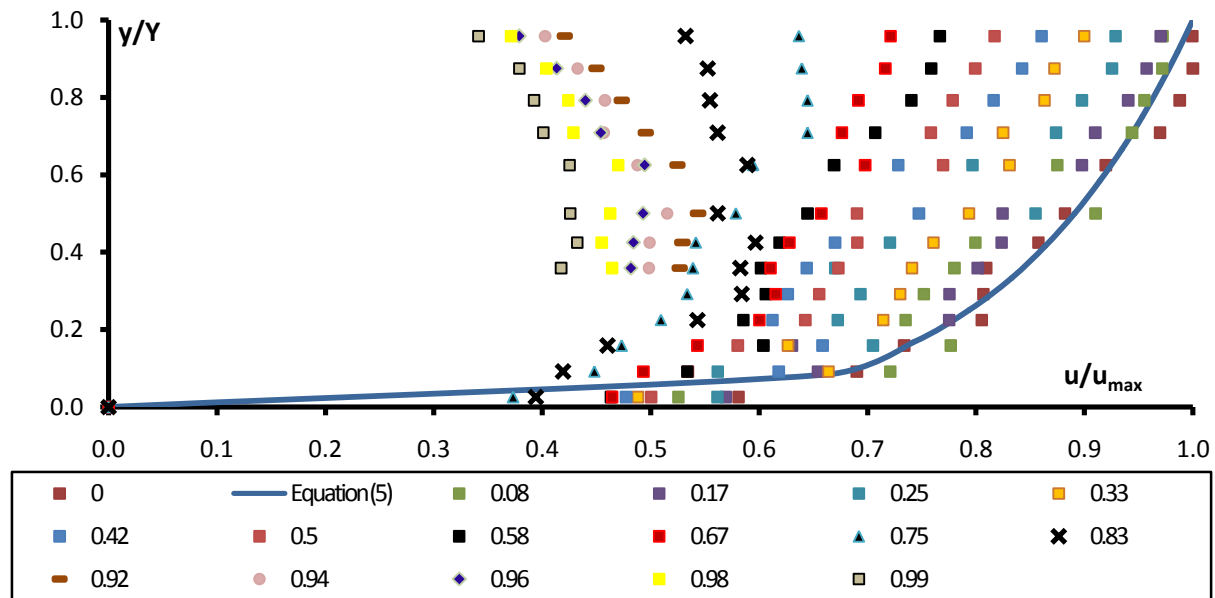


Figure no 7: Relative velocity versus relative vertical distance at different relative x , in OCF

2. **Cases of BER = 25%, 50%, and 67%:** These experiments represent the FCEB with symmetric smooth extensions. With reference to Figures no 4, 5, and 6, the following may be noticed:

- Fixed extensions are considered to be added boundaries to the flume cross section. Resulting boundary layers affect the velocity distributions forming low velocity zones (LVZ) bounded by the flume bed, the flume side wall, and the extension.
- Iso-lines of the velocity distributions in the LVZ resemble that of PF with major difference that the iso-lines in cases of LVZ of FCEB are not closed due to the absence of the fourth boundary.
- Getting closer to the centerlines, the effect of side boundaries on velocity distributions begins to vanish.

- The maximum velocities of the LVZ in the three cases are noticed to be located near the mid depth ($y \approx 0.5Y$).
- The maximum cross sectional velocities in the three cases are noticed to be located at the centerline near the surface.

Figure no 8 shows the variation of the relative centerline velocity with relative vertical distance in FCEB. The blue, brown and green markers give relative velocities at BER = 25%, 50%, and 67%, respectively. The black and red solid lines show the two limitations of equation 5 with $N = 4$ and 12 , respectively. The power trend is still valid and data matches reasonably with equation 5 for $N = 12$.

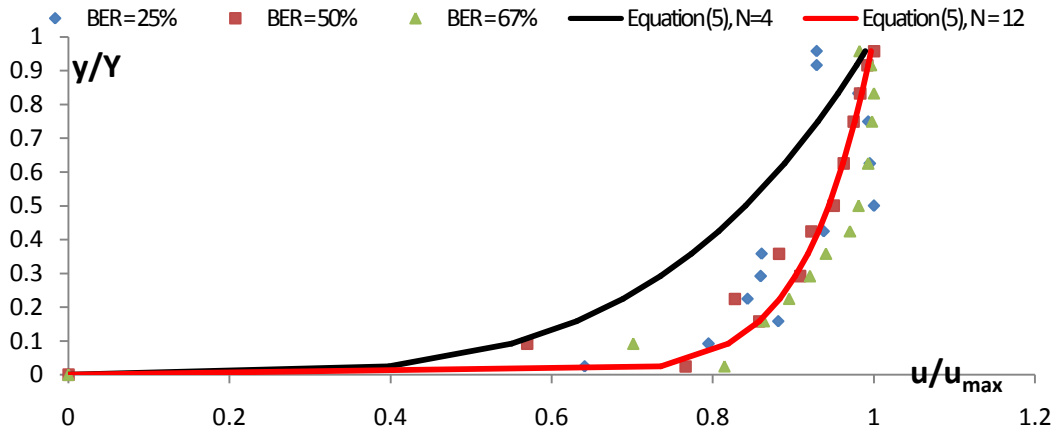


Figure no 8: Relative centerline velocity versus relative vertical distance in FCEB

3. Discharge Distribution: The discharge distribution in the flow cross section denotes the share of every part of the section in passing the flow. In FCEB, less flow discharge is allowed to pass through the LVZ. This brings about more discharges passing through the rest of the section (i.e. the uncovered part of the cross section). This matches well with Shen and Ackermann¹⁴, and Mitchel⁸ in their studies for the case of the flow area partially covered with ice layers. Using the experimental data, the discharges in the LVZ may be calculated based on the discharge definition equation:

$$Q = \int_0^A u \, dA \cong \sum_{i=1}^n u_i \Delta A_i \tag{9}$$

Where n is the number of readings.

The SURFER software was used to calculate the percentage of discharge passing through LVZ (Q_{LVZ}) in the three cases of BER = 25%, 50%, and 67% with respect to the discharge passing through half the section (Q_{hs}) and compare it to the reference case of OCF (BER = 0%). Table no 1 shows the results of the discharge distributions calculated based on the experimental data.

Table no 1: Discharge distribution

	Q_{hs} (L/s)	Q_{LVZ} (L/s)			$(Q_{LVZ}/Q_{hs})\%$		
		25%	50%	67%	25%	50%	67%
OCF	29.890	5.571	12.668	18.126	18.64	42.38	60.64
FCEB (BER = 25%)	31.600	3.565			11.28		
FCEB (BER = 50%)	35.000		13.360			38.17	
FCEB (BER = 67%)	34.870			20.173			57.85
Reduction Percentage					7.36	4.21	2.79

Results in Table no 1 show that, in case of OCF and due to the side boundary effects, the flow is not equally distributed across the flow section. The first 25% of the flow area close to the side boundary passes only 18.64% of the discharge. Going far from the boundary (closer to the centerline), the second 25% of the flow area passes 42.38% - 18.64% = 23.47% of the discharge. Then, the following 17% of the area passes 18.26%.

The existence of the fixed extensions in FCEB made the distribution even worse. The discharges passing through LVZ of the three FCEB cases with BER = 25%, 50%, and 67% are only 11.28%, 38.17%, and 57.85% of the total discharge, respectively. Compared with the reference case of OCF, the three LVZ of the three FCEB cases passed less discharges by 7.36%, 4.21%, and 2.79%, respectively.

From the practical point of view, less velocities and less discharges in the LVZ beneath the extensions, which could be any of the environmental engineering applications mentioned earlier, mean much less flow energy in these zones. The consequences would be accumulation of dirt and weeds, existence of bad smells due to unexpected non-desirable chemical reactions, and more probabilities of sedimentation. That is why the engineer should perform purification of water in LVZ as part of his management for this engineering application especially if it was constructed for recreation purposes.

V. Summary And Conclusion

In this paper, the flow in channels with extended boundaries (FCEB) was introduced. In FCEB, the channel boundaries are extended to cover part of the free surface. From the hydraulic point of view, the extensions just touch the flow, so the pressure on the top surface is still *approximately* atmospheric, and both the velocity and discharge distributions are affected. Some of the flow characteristics of FCEB and some of its field engineering applications were outlined with stresses on the hydraulic differences between this type of flow and both pipe flow (PF) and open channel flow (OCF). Laboratory experiments were conducted to investigate three cases with different BER of smooth symmetric extensions and the case of OCF for comparison using ADV sampling.

For the case of OCF, results showed that the height of the boundary layer is very small, the effect of the side boundaries is negligible, and the variation of the relative velocity with relative vertical distance at the centerline matches well with the Prandtl power law (for $N = 6$). Starting from the side boundaries, the discharge distribution showed that the parts near the centerline pass more flow discharges. The first 25% of the flow area, close to the side boundary, passes only 18.64% of the discharge.

In FCEB, (experiments with BER = 25%, 50%, and 67%), low velocity zones (LVZ) are formed in the part covered with the extensions with velocity distribution resembling the PF case, but the FCEB iso-lines are not closed. The maximum velocities of the LVZ in the three cases are noticed to be located near the mid depth. For the variation of the relative velocity with relative vertical distance at the centerline, the power trend is valid and data matches reasonably with equation 5 for $N = 12$.

Symbols and Abbreviations

a	Aspect ratio = b/Y	LDA	Laser Doppler Anemometer
ADV	Acoustic Doppler Velocimeter	LVZ	Low Velocity Zone
b	Channel bed width	n and N	Number of readings and Power Law exponent, respectively
BER	Boundaries Extension Ratio	OCF	Open Channel Flow
C_1, C_2, C_3, C_4	Constants defined elsewhere	PF	Pipe Flow
F	Froude number	Q	Discharge
FCEB	Flow in Channels with Extended Boundaries	u, u_s, u_{max}, U	Flow velocity, Shear velocity, Maximum velocity, and Average Velocity, respectively
HDOP	High Dense Overlay Plywood	X1, X2	Widths of extensions
k	Von-Karman constant	x, y, y/Y	Distance from centerline, Vertical distance, Vertical distance at $u = 0$, and Flow depth, respectively
k_s	The roughness height	v	Kinematic viscosity

References

- [1]. Chanson H., "Open Channel Flow", in Environmental Hydraulics of Open Channel Flows, 2004. Published by online Sciencedirect/ Elsevier, <https://www.sciencedirect.com/topics/earth-and-planetary-sciences/open-channel-flow/pdf>
- [2]. Chen C.L., "Unified theory on power laws for flow resistance", J. of Hydraulic Engineering, ASCE, Vol. 117, No. 3, March 1991, pp. 371-389
- [3]. González J., Melching C., and Oberg K., "Analysis of Open-Channel Velocity Measurements Collected with an Acoustic Doppler Current Profiler" Reprint from RIVERTECH 96. Proceedings from the 1st Int. Conf. on New Emerging Concepts for Rivers Organized by the Int. Water Resources Association held in September 22-26, 1996, Chicago, Illinois, USA
- [4]. Kamal M., "Laboratory and MatLab programming techniques in ADV measurements", M.Sc. Thesis, Faculty of Engineering, Ain Shams University, Cairo, Egypt, 2018.
- [5]. Kumbhakar M., Ghoshal K., and Singh V., "Two-dimensional distribution of streamwise velocity in open channel flow using maximum entropy principle: Incorporation of additional constraints based on conservation laws", J. Computer Methods in Applied Mechanics and Engineering, Vol. 3611 April 2020, Article 112738.
- [6]. Kundu S. and Ghoshal K., "Velocity distribution in open channels: Combination of Log-law and Parabolic-law", World Academy of Science, Engineering and Technology, Vol. 68 2012-08-23, pp 2151-2158. Uploaded by Kundu on ResearchGate on 20 January 2014.
- [7]. Lassabatereb L., Hui Puc J., Bonakdarid H., Joannise C., and Larrarte F., "Velocity distribution in open channel flows: An analytical approach for the outer region", J. of Hydraulic Engineering, January 2013. Uploaded by Larrarte on ResearchGate on 18 August 2016.
- [8]. Mitchel R., "An experimental study of the hydraulic characteristics beneath a partial ice cover", M.Sc. Thesis, Water Resources Group, University of Manitoba, Canada, 2015
- [9]. Monteroa V, Romagnolib M, Garcia M, Canterod M, and Scacchie G, "Optimization of ADV sampling strategies using DNS of turbulent flow", J. of Hydraulic Research, Vol. 52, No. 6, 2014, pp. 862-869.

- [10]. Nezu I., and Rodi W., “Experimental study on secondary currents in open channel flow”, Proc., 21st Congress of IAHR, Melbourne, Australia, Vol. 2, 1985, pp. 115-119.
- [11]. Pradhan A., Khatua K., and Sankalp S., “Variation of velocity distribution in rough meandering channels”, Hindawi Advances in Civil Engineering, Vol. 2018, Article 1569271, <https://doi.org/10.1155/2018/1569271>
- [12]. Rasoul J., Anagnostopoulos P., and Ganouls J., “Numerical and experimental investigation of laminar flow through a staggered bundle of cylinders”, J. of ZAMM Z. angew. Math. Mech. 74, 1994, pp 333-340 (In English with German abstract).
- [13]. Ruonan B., Liekai C., Xingkui W., and Danxun L., “Comparison of ADV and PIV measurements in open channel flows”, 12th International Conf. on Hydroinformatics, HIC 2016, Science Direct, Procedia Engineering 154, 2016, pp 995 – 1001.
- [14]. Shen, H.T. and Ackermann, N.L., “Wintertime flow Distribution in river channels”, J. Hydraul. Div. ASCE, 106(HY5), 1980, pp. 805-817.
- [15]. Tang T. and Davar K., “Resistance to flow in partially covered channels”, Proc. 2nd Workshop on the Hydraulics of Ice covered rivers, Edmonton, Alberta, Canada, 1982, pp 232-252.
- [16]. Voulgaris G. and Trowbridge J., “Evaluation of the Acoustic Doppler Velocimeter (ADV) for turbulence measurements”, J. of Atmospheric and Oceanic Technology, American Meteorological Society, Vol. 15, pp 272-289, 1998.
- [17]. Yang Y., Wen B., Wang C., and Hou Y., “Two-dimensional velocity distribution modeling for natural river based on UHF radar surface current”, J. of Hydrology, Vol. 577, October 2019, Article No. 123930.

M. Kamal, et al. “Experimental Investigation of Flow in Channels with Extended Boundaries.”
IOSR Journal of Mechanical and Civil Engineering (IOSR-JMCE), 17(2), 2020, pp. 01-10.